

An Analytical Solution to the Transient One-Dimensional Compressible Pipe-Flow Equations

Andrew P. L. Newton, Senior Scientist, Health and Safety Executive (HSE), Harpur Hill, Buxton, SK17 9JN, UK
andrew.newton@hse.gov.uk

Modelling transient mass release rates from transmission pipelines is an important part of hazard assessments for safety, environmental protection, and regulatory compliance. An understanding of transient flow dynamics can help regulators, operators and emergency responders better assess potential hazards, optimise mitigation measures and minimize the impact of accidental releases.

Models capable of predicting the transient decompression behaviour of full-bore ruptures of pipelines transporting compressible fluids are generally very complex and difficult to implement. There is considerable value in developing simple and reliable tools which are easy to deploy, may be used in consequence models, or that can be used as a method to verify more complex solutions.

As part of the UK Health and Safety Executive's (HSE) work developing and updating the tools used to regulate major accident hazard pipelines, an analytical solution to the conservation equations describing compressible pipe-flow has been derived which is applicable to the full-bore/guillotine rupture scenario. The resulting tool (PolyPiRRaM, Polytropic Pipeline Release Rate Model) is simple to implement, identifies fundamentally new pipeline behaviour and can be used to model accidental releases which are initially pressure liquefied, supercritical or gaseous.

PolyPiRRaM is derived from the quasi-steady compressible pipe-flow equations, which can be applied almost seamlessly to a wide range of fluids. The new model predicts that all compressible pipeline decompression exhibits universal behaviour in the earliest stage of the release, where a stationary zone in the pipe is present.

The decompression in the later stages of a release is sensitive to the material properties, specifically the polytropic index, m, and previous analytical results are recovered in the long-time limit. The polytropic index allows the density to be expressed as a power law function of pressure, the initial pressure and the initial density. It is found by numerically evaluating an integral along an isenthalpic trajectory using a real gas equation of state.

The only free parameter in the model is the pipe exponent n which links the mass flux density in the expanding zone with the local co-ordinate and length to the mass flux density at the end of the pipe. However, n is set according to the values that are already known to be suitable from PiRRaM (the HSE pipeline model for pressure liquefied fluids), and DNV's PipeBreak and GasPipe models. As n is presumed to be known a-priori, the model makes predictions without the possibility or need for calibration.

The new model predicts transient mass release rates for full-bore ruptures to pipelines, across a wide range of scenarios. PolyPiRRaM can be applied to releases of pressure liquefied substances (ammonia, dense phase carbon dioxide, ethylene, cryogenic liquid hydrogen, and propane) and gas releases (natural gas, light phase carbon dioxide, and hydrogen at ambient temperatures). The application is not restricted to pipelines on land, as subsea releases can be modelled provided the water depth is sufficiently shallow.

Keywords: PiRRaM, MISHAP, HSE, pipeline modelling, holes, pressure liquefied gas, carbon dioxide, ammonia, hydrogen, MAH pipelines

Introduction

This paper describes a novel calculation which was performed during the routine maintenance and development of the Health and Safety Executive's (HSE) MISHAP computer model (Model for the estimation of Individual and Societal risk from HAzards of Pipelines). MISHAP is used to calculate the risks to people, and ultimately the land-use planning (LUP) zones from Major Accident Hazard (MAH) pipelines carrying flammable substances. An earlier paper (Newton, 2022) reported on the development of PiRRaM, the Pipeline Release Rate Model, which is used in MISHAP to predict the transient mass flow rate from accidentally ruptured pipelines transporting pressure liquefied fluids.

The model described in this paper is notable in that it is capable of modelling both gas and pressure liquefied fluid outflow, and it may even be possible to develop a framework to account for supercritical conditions. It is this broad generalisation that allows the dynamics of a range of transient compressible pipe flow to be modelled.

This paper starts by reviewing the options available for modelling pipeline decompression before briefly describing the experimental data which is available to validate the model. The quasi-steady compressible pipe-flow equations and other general principles of modelling transient pipeline releases are then described, followed by an introduction to the approximate equation of state. The derivation of the model is then described, which starts with a series of calculations characterising the properties of a generalised expanding zone. Results from the expanding zone calculation are then used to elicit solutions to the early and late time regimes respectively. A discussion of the technical aspects of implementing the model is then provided.

Model testing is then described, including an analysis performed using gaussian emulation modelling to ascertain the sensitivity of model predictions to uncertainty in input variables, and a model intercomparison exercise. With assurances from the model testing activities that the equations are accurately implemented, validation comparisons to a series of gas and pressure liquefied fluid experiments are then performed. A discussion summarising the limitations and wider applicability of the new technique is then presented.

Review of Existing Pipeline Decompression Models

Newton (2022) provides a detailed review of the background literature and other available models, and the reader is directed there for a comprehensive overview of the relevant research. Of particular interest is the work on pure gas releases reported in Fannelop and Ryhming (1982). In that work, an integral-type model for full guillotine ruptures of pipelines transporting gases is derived analytically from the one-dimensional conservation equations for mass, momentum and energy, corresponding to compressible pipe flow. Fanneløp and Rhyming (1982) split the pipe into an expanding and stationary zones, and use the ideal gas equation of state to find a solution for the later time regimes where the entire contents of the pipe are in motion.

The technique of modelling the pipe as separate zones has been widely adopted and forms the basis of pipeline models in several independent tools including HSE's PiRRaM, PipeBreak and GasPipe in DNV's PHAST, Shell's FRED and AspenTech's BlowDown (Newton, 2022). The advantage of this technique is that it enables computationally efficient methods to be developed that allow pipe decompression to be modelled with acceptable accuracy for consequence modelling activities.

The development of tools which are quick to run, whilst providing useful insights into the underlying phenomena, has been a continual objective in process safety engineering. Since the earliest experiments on pressure liquefied fluid releases, efforts have been made to produce simple models describing the key characteristics (Tam & Higgins, 1990). More recently, several additional novel tools have been developed to model pipeline phenomena. Yu et al. (2024) developed a small hole model for saturated two-phase releases of carbon dioxide where the flow is likely to be stratified. Martynov et al. (2024) manipulated the quasi-steady compressible flow equations into a nonlinear diffusion equation in pressure. This form is particularly amenable to numerical analysis and enables the development and assurance of a simplified model for pipeline packing, which is the process of increasing product in a pipeline to maximise capacity and ensure efficient operation. .

One method for analysing the characteristics of pipeline accidents has been the Bell equation. Bell (1978) proposed a technique based upon an empirical double exponential decay function, which was later adapted by Wilson (1979 (Re-issued 1986)). The resulting phenomenological model unites physically sound ideas in a non-rigorous manner to characterise a complex phenomenon in a relatively simple way. For example, the choked isentropic ideal gas equations are used to model the initial mass flow rate, and steady state compressible gas pipe-flow calculations are used to infer the transient fluid flow behaviour. The reliability of such an approach depends on how successfully the underlying physics are chosen and represented in the model. The inherent simplicity of the resulting approach made the model popular and it has been widely adapted (Wilson, 1979; Chaplin, 2015) and adopted into several software packages, including ALOHA (Jones et al., 2013), FRED (Betteridge, 2023) and MISHAP (Chaplin, 2015). The approach has also been recommended in Lees (2012) and the Yellow Book (Van den Bosch & Weterings, 2005). Zelensky and Zelt (2010) assert that the dependence of the initial decay, predicted by the Bell equation, on the later steady state indicates that the double exponential form of the Bell equation cannot be correct.

Experimental Data

The experimental data identified in Newton (2022) for pressure liquefied fluids is supplemented with experiments where the working fluid is gaseous. This is not an exhaustive examination of the literature. However, these experiments provide sufficient evidence to demonstrate the performance of the model for gas releases. Table 1 and

Identifier	Material	Pipe Length (m)	Pipe Diameter (mm)	Temperature (°C)	Pressure (bar)
NorrisFBR	Methane	609.6	10.21	5	119
APIGEC7	Air	1987	157.18	5	71
APIGEC2	Air	3438	305	5	69.4

Table 2 summarise the key characteristics of the validation datasets for gas and pressure liquefied releases respectively. A more detailed discussion of the datasets is given below.

The Alberta Petroleum Industry Government Environmental Panel (APIGEC, 1979) undertook a series of studies aimed at evaluating the available techniques used to define potentially hazardous zones in the vicinity of sour gas operations (natural gas with a significant proportion of hydrogen sulphide). In all, 33 experiments were performed releasing high-pressure air from either a 4 km long 157 mm inner diameter pipe or a 7.1 km long 305 mm inner diameter pipe. Tabulated mass flow rate data is presented for 3 experiments where measurements are given for the releases on a single side of the release (corresponding to approximately half the pipe length). Of the three experiments for which tabulated data is available, trials 7 and 22 are selected for inclusion here.

Norris (1994) describes 15 gas releases, using three gas mixtures, from a reduced scale pipeline. The experimental pipeline was 609.6 m long with an internal diameter of 10.21 mm, and the experiments released gas through nozzles ranging from 2.4% to 100% of the pipe area. The experiments were designed to reproduce realistic length to diameter ratios. An equivalent full-scale pipe with an internal diameter of 150 mm would be approximately 9 km long. The full-bore rupture experiment using natural gas is chosen to validate the model.

The Isle of Grain trials (Richardson & Saville, 1996), released propane from 100 m long pipes in various configurations. Of particular interest here are the full-bore rupture releases from the 150 mm and 50 mm diameter pipe performed during trials P40 and P61 respectively. These experiments were well instrumented and have been widely used to validate several pipeline decompression models.

Table 1 Summary of gas experiments for validation dataset

Identifier	Material	Pipe Length (m)	Pipe Diameter (mm)	Temperature (°C)	Pressure (bar)
NorrisFBR	Methane	609.6	10.21	5	119
APIGEC7	Air	1987	157.18	5	71
APIGEC2	Air	3438	305	5	69.4

Table 2 Summary of pressure liquefied fluid experiments for validation dataset

Identifier	Material	Pipe Length (m)	Pipe Diameter (mm)	Temperature (°C)	Pressure (bar)
IoG P40	Propane	100	150	17.8	21
IoG P61	Propane	100	50	15	21

PolyPiRRaM Derivation

Overview

The new model follows Fannelop and Ryhming (1982) and Webber et al. (1999) in assuming that the momentum and energy conservation equations are slowly evolving, and that the convective acceleration is negligible (due to the absence of shocks significantly affecting the calculation). The equations describing the quasi-steady one-dimensional compressible flow along a pipe are given below for the mass, momentum, and energy conservation respectively:

$$\frac{\partial \rho}{\partial t} + \frac{\partial G}{\partial x} = 0, \qquad \frac{\partial P}{\partial x} = -\frac{2fG|G|v}{D_{\text{pipe}}} \qquad \text{and} \qquad h = \text{constant}. \tag{1}$$

Where ρ is the fluid density (kg m^{-3}), t is the time (s), G is the mass flux density (kg/m^2/s), v is the specific volume (m^3 kg^{-1}); x is the location along the pipe (m), P is the pressure (Pa), f is the Fanning friction factor (-), D_{pipe} is the pipe diameter (m) and h is the specific enthalpy (J/kg). In the new model, solutions to these equations are sought for horizontal and straight pipes containing fluids which are initially stationary with a uniform pressure along the pipe. These conditions are chosen to simplify the problem whilst also representing a justifiably conservative option.

The pipeline decompression is modelled as evolving through two flow regimes: an early time regime where the pipe has a stationary and expanding zone, and a late time regime where the entire contents of the pipe are in motion and the expanding zone fills the entire pipe. In this case the solutions derived in the next section can be adapted to represent each scenario through changing the limits of integration or by fixing the length of the expanding zone to be the pipe length. To mathematically describe the early and late time regimes, it is convenient to include a transition case which corresponds to the point at which the solution switches between the early and late time regimes. These different scenarios are shown in Figure 1 (overleaf), where blue indicates undisturbed stationary fluid at the initial pressure, and the yellow to red represents the pressure change as the gas expands down the pipe (yellow and red corresponding to high and low pressure respectively).

The model derivation requires a thorough characterisation of the expanding zone. This algebraically links the mass flux density at the end of the expanding zone to the pressure profile in the zone, the length of the expanding zone and its total mass. The early time regime then calculates the total pipe inventory as the sum of a stationary zone, with uniform density and pressure, and an expanding zone. The late time regime evaluates the expanding zone between the exit pressure and an upstream pressure which is less than the initial pressure. The transition case corresponds to the scenario where the length of the modelled expanding zone exactly matches the length of the pipe.

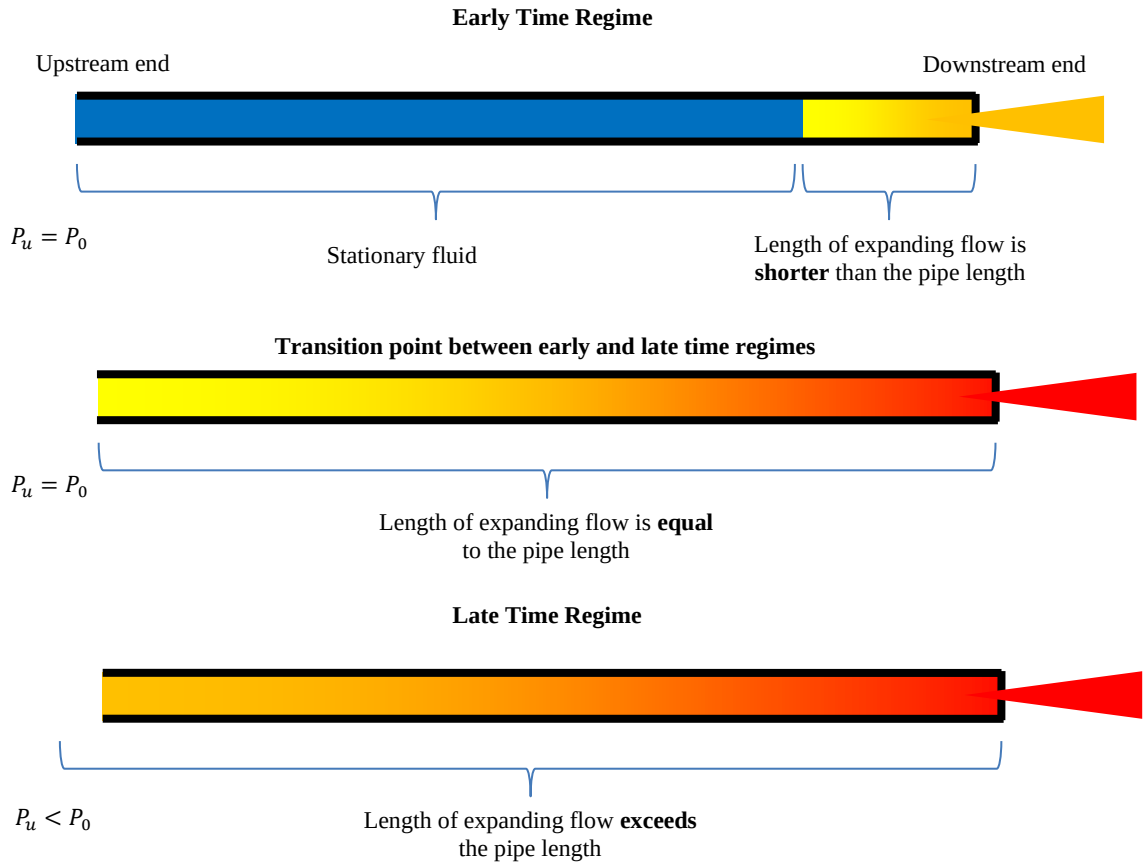

Figure 1 Schematic showing early time regime (top), the late time regime (bottom) and the transition point between them (middle).

Polytropic Equation of State

A polytropic equation of state[1] relating the pressure and density of a fluid is assumed to have the following relationship:

$$\rho = \rho_0 \left(\frac{P}{P_0}\right)^m . \tag{2}$$

Where P is the pressure (Pa), ρ is the fluid density (kg/m^3);,); m is the polytropic index[2] (dimensionless) and K is a constant of proportionality (dimensionless). The subscript 0 relates to stagnation conditions before the pipe is opened, and m is a constant which is found numerically to satisfy a momentum conservation integral. The above is therefore used as an approximation to an accurate equation of state that has the properties of matching the initial density and satisfying an important momentum conservation integral which is introduced later.

Momentum Conservation

An axial co-ordinate system X^* is defined relative to the expanding zone such that $X^* = 0$ corresponds to the upstream end of the expanding zone, and $X^* = L_{\text{expd}}$ corresponds to the point where the fluid leaves the pipe. This allows the following power-law profile to be assumed for the mass flux density in the expanding zone:

[1] See the footnote in Landau and Lifschitz,(1991) on page 318: *"The name polytropic is derived from polytropic process, i.e. one in which the pressure varies as some power of volume"*.

[2] Here, the polytropic index (m) is defined for convenience via $\rho = \rho_{0_0}(PP_0^{-1})^m$. (2), which is similar to other authors who define m to relate pressure (P) and volume (V) during a process via $PV^m = C$, where C is a constant, which corresponds to a relationship $P = P_0(\rho\rho_0^{-1})^m$.

$$G(X^*,t) = \left(\frac{X^*}{L_{\text{expd}}(t)}\right)^n G_{\text{d}}(t). \tag{3}$$

Where G_{d} is the mass flux density of the fluid leaving the pipe (kg/m^2/s), X^* is the new co-ordinate relative to the expanding zone (m), L_{expd} is the length of the expanding zone (m) and n is the pipe flow index (-). The pipe flow index is chosen using pre-existing values which have previously been used for pressure liquefied flow ($n = 0$, PipeBreak/PiRRaM) and expanding gas flows ($n = 2$, PHAST's GasPipe). The $n = 0$ value corresponds to a uniform mass flux density in the pipe, whereas $n = 2$ indicates a parabolic relationship between the mass flux density and its position in the expanding zone. Practically, these values along with the polytropic index (m) determine the average density in the expanding zone. Equation (3) has the property of being zero when $X^* = 0$ at the upstream end of the expanding zone, and matching the outlet mass flux density, $G\big(L_{\text{expd}}(t),t\big) = G_{\text{d}}(t)$, at the downstream end of the expanding zone.

The polytropic approximation (2) and the assumed mass flux density profile (3) are substituted into the momentum conservation equation (1). The resulting equation is integrated from an arbitrary position in the expanding zone ($X^* = X$) to the end of the pipe ($X^* = L_{\text{expd}}$), which corresponds to the pressure between ($P(X)$) and (P_d). Noting that $G_{\text{d}} > 0$ (i.e. velocity in the positive X^* direction the following relationship is obtained

$$\frac{\rho_0}{P_0^m}\int_{P(X)}^{P_d} P^m dP = -\frac{2f}{D_{\text{pipe}}}\frac{G_{\text{d}}^2}{L_{\text{expd}}^{2n}}\int_{X}^{L_{\text{expd}}} X^{*2n}\, dX^*. \tag{4}$$

This is integrated assuming[3] that $P_{\text{d}} \ll P_0$ to get the following expression for the pressure at a location X in the expanding zone:

$$P(X) \approx P_0\left(\frac{2fG_{\text{d}}^2}{P_0\rho_0 D_{\text{pipe}}}\frac{m+1}{2n+1}L_{\text{expd}}\left[1-\left(\frac{X}{L_{\text{expd}}}\right)^{2n+1}\right]\right)^{\frac{1}{m+1}} \tag{5}$$

Setting $X = 0$ and $\text{P}(X^* = 0) = P_0$, the length of the expanding zone is given by:

$$L_{\text{expd}} = \frac{P_0\rho_0\, D_{\text{pipe}}}{2fG_{\text{d}}^2}\frac{2n+1}{m+1}. \tag{6}$$

Equation (5) also allows the mass in the expanding zone (M_{expd}) to be calculated as integral of density over its length. Using the approximate polytropic equation of state (2), the mass in the expanding zone is given by:

$$\frac{M_{\text{expd}}}{A_{\text{pipe}}} = \int_0^{L_{\text{expd}}} \rho\big(P(X^*)\big)\, dX^* = \int_0^{L_{\text{expd}}} \rho_0\left[1-\left(\frac{X^*}{L_{\text{expd}}}\right)^{2n+1}\right]^{\frac{\text{m}}{m+1}} dX^* \tag{7}$$

Which with a change of variable, $x^* = \frac{X^*}{L_{\text{expd}}}$, becomes

$$\frac{M_{\text{expd}}}{L_{\text{expd}}A_{\text{pipe}}\rho_0} = \frac{\bar{\rho}}{\rho_0} = \int_0^1 \left(1-x^{*2n+1}\right)^{\frac{m}{m+1}} dx^* = \frac{\Gamma\left(1+\frac{1}{2n+1}\right)\Gamma\left(1+\frac{m}{m+1}\right)}{\Gamma\left(1+\frac{1}{2n+1}+\frac{m}{m+1}\right)}. \tag{8}$$

Where $\bar{\rho}$ is the average density in the expanding zone and $\Gamma(x)$ represents the gamma function, which is a mathematical function which extends the concept of the factorial function to non-integer real and complex numbers. Fortunately, libraries exist which enable its robust and efficient calculation.

Analytical Solution to the Early Time Regime

In the early time regime, the length of the expanding zone (L_{expd}) is less than the pipe length (L_{pipe}) in which case the mass in the pipe consists of a stationary zone with length $L_s = L_{\text{pipe}} - L_{\text{expd}}$, and an expanding zone of length L_{expd}. An equation for the mass in the pipe can again be derived as the sum of the stationary and expanding zones as:

[3] After the pipe is opened the pressure at the release plane will quickly drop to atmospheric pressure. In this case, it is reasonable to assume that $P_{\text{d}} \ll P_0$ to elicit a convenient solution.

$$M_{\text{pipe}} = M_s + M_{\text{expd}} = A_{\text{pipe}}\left(L_{\text{pipe}} - L_{\text{expd}}\right)\rho_0 + A_{\text{pipe}}L_{\text{expd}}\bar{\rho} \tag{9}$$

Where in addition to the previously defined variables, M_s and M_{expd} correspond to the stationary and expanding zones of flow respectively, and $\bar{\rho}$ is the average density in the expanding zone calculated from (8). Noting that the initial mass in the pipe (M_0,kg) is given by $M_0 = \rho_0 A_{pipe} L_{pipe}$, and substituting the equation for the length of the expanding zone (6) into (9), gives

$$\frac{M_0 - M_{\text{pipe}}}{A_{\text{pipe}}} = \frac{\rho_0 P_0\, D_{\text{pipe}}}{2fG_{\text{d}}^2}\frac{2n+1}{m+1}(\rho_0 - \bar{\rho}). \tag{10}$$

At which point, the equation for mass conservation (1) can be integrated along the pipe to provide a relationship between the mass in the pipe and the mass flux density of the fluid leaving the pipe (G_{d}). Specifically, integrating the mass conservation equation (1) along the pipe whilst assuming zero inflow reveals the relationship[4]:

$$\frac{dM_{\text{pipe}}}{dt} = -A_{\text{pipe}}G_{\text{d}}. \tag{11}$$

Substituting this into equation (10) gives the following differential equation:

$$\left(M_0 - M_{\text{pipe}}\right)\left(\frac{dM_{\text{pipe}}}{dt}\right)^2 = \beta, \text{where } \beta = A_{\text{pipe}}^3\frac{\rho_0 P_0\, D_{\text{pipe}}}{2f}\frac{2n+1}{m+1}(\rho_0 - \bar{\rho}) \tag{12}$$

This is an ordinary differential equation is solved by the separation of variables technique revealing the following solution for an initial condition $M_{\text{pipe}}(0) = M_0$:

$$M_{\text{pipe}} = M_0 - t^{\frac{2}{3}}\left(\frac{9}{4}\beta\right)^{\frac{1}{3}}, \text{and } \left|\frac{dM_{\text{pipe}}}{dt}\right| = \frac{2}{3}t^{-\frac{1}{3}}\left(\frac{9}{4}\beta\right)^{\frac{1}{3}}. \tag{13}$$

This is particularly novel, as the scaling law is predicted to be a ubiquitous property of compressible flow escaping pipelines during the early stages of the release. Specifically, the mass flow rate ($\dot{M}$) is predicted to decay to the minus one-third power of time ($\dot{M} \propto t^{-\frac{1}{3}}$) when the flow can be characterised as having both expanding and stationary zones. Moreover, the mass flow rate is predicted to halve when the time after the release is eight times longer (i.e. if the mass flow rate is 100kg/s at 10 s after the rupture, it will reach 50 kg/s at 80 s after the rupture).

Analytical Solution to the Late Time Regime

To derive an equation for the inventory in the pipe for the late time regime, we return to the pressure profile (5), this time noting that the length of the expanding zone is limited to the length of the pipe ($L_{\text{expd}} = L_{\text{pipe}}$) and seeking the upstream pressure (P_{u}):

$$P_{\text{u}} = P_0\left(\frac{2fG_{\text{d}}^2}{\rho_0\, P_0 D_{\text{pipe}}}\frac{m+1}{2n+1}L_{\text{pipe}}\right)^{\frac{1}{m+1}}. \tag{14}$$

Which enables the upstream density to be calculated as:

$$\rho_{\text{u}} = \rho_0\left(\frac{2fG_{\text{d}}^2}{\rho_0\, P_0 D_{\text{pipe}}}\frac{m+1}{2n+1}L_{\text{pipe}}\right)^{\frac{m}{m+1}}. \tag{15}$$

As before, we integrate the density profile along the pipe, between the downstream pressure, which is assumed to provide a negligible contribution, and the upstream pressure:

$$M_{\text{pipe}} = A_{\text{pipe}}L_{\text{pipe}}\bar{\rho}^* \tag{16}$$

[4] If pumped inflow is required, the resulting differential equation is analytically solvable, but the solution does not give the mass as an explicit function of time. Moreover, the effect of liquid compressibility can be modelled by including a source term $A_{pipe}c_{sound}(\rho_0 - \rho_{sat})$ for a finite length pipe, or $A_{pipe}c_{sound}(\rho_0 - \rho_{sat})/2$ for an infinite pipe. In which case, the inclusion of pumping or the effect of liquid compressibility into the model is possible but is not done here for brevity.

Noting that the pipe averaged density in the late time regime ($\bar{\rho}^*$) is defined slightly differently. Using a change of variables ($x^* = X^* L_{\text{pipe}}^{-1}$), $\bar{\rho}^*$ is related to $\bar{\rho}$ via:

$$\bar{\rho}^* = \rho_u \int_0^1 \left(1 - x^{*2n+1}\right)^{\frac{m}{m+1}} dx^* = \frac{\rho_u}{\rho_0} \bar{\rho}. \tag{17}$$

Remembering that upstream density is already calculated (15), we can substitute the pipe average density (17) into the equation for the mass in the pipe (16), whilst reusing the mass conservation relationship (11) to get:

$$M_{\text{pipe}} = A_{\text{pipe}} L_{\text{pipe}} \rho_0 \left[\frac{2f}{\rho_0 P_0 D_{\text{pipe}} A_{pipe}^2} \left(\frac{dM_{\text{pipe}}}{dt} \right)^2 \frac{m+1}{2n+1} L_{\text{pipe}} \right]^{\frac{m}{m+1}} \times \int_0^1 \left(1 - x^{*2n+1}\right)^{\frac{m}{m+1}} dx^*. \tag{18}$$

Noting that the mass in the pipe at the point of transition (M_{trans}) between the early and late time regimes occurs when the mass in the pipe is given by:

$$M_{\text{trans}} = A_{\text{pipe}} L_{\text{pipe}} \rho_0 \int_0^1 \left(1 - x^{*2n+1}\right)^{\frac{m}{m+1}} dx^* = A_{\text{pipe}} L_{\text{pipe}} \bar{\rho}. \tag{19}$$

Where $\bar{\rho}$ is defined in (8). The equation for the inventory mass (18) can then be simplified:

$$M_{\text{pipe}} = M_{\text{trans}} \left[\frac{2f}{\rho_0 P_0 D_{\text{pipe}} A_{pipe}^2} \left(\frac{dM_{\text{pipe}}}{dt} \right)^2 \frac{m+1}{2n+1} L_{\text{pipe}} \right]^{\frac{m}{m+1}}. \tag{20}$$

Taking the negative root, corresponding to mass leaving the pipe, gives the differential equation for the pipe inventory mass:

$$M_{\text{pipe}}^{-\frac{m+1}{2m}} \frac{dM_{\text{pipe}}}{dt} = -M_{\text{trans}}^{-\frac{m+1}{2m}} \sqrt{\frac{\rho_0 P_0 A_{\text{pipe}}^2 D_{\text{pipe}}}{2f L_{\text{pipe}}} \frac{2n+1}{m+1}} \tag{21}$$

Which is expressed more conveniently by introducing a constant ($\dot{M}_{\text{trans}}$), the mass flow rate at the point of transition between the early and late time flow regimes, as:

$$M_{pipe}^{-\frac{m+1}{2m}} \frac{dM_{\text{pipe}}}{dt} = -M_{\text{trans}}^{-\frac{m+1}{2m}} \dot{M}_{\text{trans}}, \text{where } \dot{M}_{\text{trans}} = A_{pipe} \sqrt{\frac{\rho_0 P_0 D_{\text{pipe}}}{2f L_{\text{pipe}}} \frac{2n+1}{m+1}}. \tag{22}$$

This is integrated, using the boundary condition $M_{\text{pipe}}(t_{\text{trans}}) = M_{\text{trans}}$, to reveal the following solutions:

$$M_{\text{pipe}} = \begin{cases} M_{\text{trans}} e^{-M_{\text{trans}}^{-1} \dot{M}_{\text{trans}} (t - t_{\text{trans}})} & m = 1 \\ M_{\text{trans}} \left(1 - \frac{m-1}{2m} \frac{\dot{M}_{\text{trans}}}{M_{\text{trans}}} (t - t_{\text{trans}}) \right)^{\frac{2m}{m-1}} & m \neq 1 \end{cases} \tag{23}$$

which, when differentiated with the absolute value taken, reveals the transient equation for the mass release rate:

$$\left| \frac{dM_{\text{pipe}}}{dt} \right| = \dot{M}_{\text{trans}} \left(\frac{M_{\text{pipe}}}{M_{\text{trans}}} \right)^{\frac{m+1}{2m}} = \begin{cases} \dot{M}_{\text{trans}} e^{-M_{\text{trans}}^{-1} \dot{M}_{\text{trans}} (t - t_{\text{trans}})} & m = 1 \\ \dot{M}_{\text{trans}} \left[1 - \frac{m-1}{2m} \frac{\dot{M}_{\text{trans}}}{M_{\text{trans}}} (t - t_{\text{trans}}) \right]^{\frac{m+1}{m-1}} & m \neq 1 \end{cases} \tag{24}$$

Implementation of Solution

The Fanning friction factor is calculated using the Haaland correlation (Haaland, 1981). The conservation equations assume that the specific enthalpy (h) remains fixed during the decompression, that is, the decompression is assumed to be isenthalpic. For ideal gases, an isenthalpic process is also isothermal, and solutions to the conservation equations have been found in the later time regime Fannelop and Ryhming (1982). Similarly, for saturated two-phase flows, isenthalpic decompression has been successfully applied in PipeBreak and PiRRaM. The question which remains is how the polytropic index (m) is best calculated.

PolyPiRRaM uses the opensource thermodynamics library CoolProp (Bell et al., 2014), to obtain accurate equation of state data for pure substances. CoolProp predictions for isenthalpic decompressions of fluids are approximated by polytropic equations of state specifying that the initial density matches the CoolProp prediction, whilst also demanding that the integral of the density with respect to pressure of the polytopic approximation recovers the CoolProp prediction:

$$\int_{P_0}^{P_{\mathrm{atm}}} \rho_{\mathrm{CoolProp}}(h_0, P)dP = \int_{P_0}^{P_{\mathrm{atm}}} \rho_0 \left(\frac{P}{P_0}\right)^m dP = \frac{\rho_0 P_0^{-m}}{m+1}\left[P^{m+1}\right]_{P_0}^{P_{\mathrm{atm}}} \xrightarrow[P_{\mathrm{atm}} \ll P_0]{} -\frac{\rho_0 P_0}{m+1}. \tag{25}$$

The right-hand side can be evaluated analytically to reveal the approximate polytropic index of this process. From which the following explicit[5] equation for the polytropic index (m) is found:

$$m = \frac{\rho_0 P_0}{\int_{P_{\mathrm{atm}}}^{P_0} \rho_{\mathrm{CoolProp}}(h_0, P)dP} - 1. \tag{26}$$

Figure 2 shows comparisons of the CoolProp predictions[6] and the polytropic approximations, for the isenthalpic decompression trajectories for propane at 40 bar (left), carbon dioxide at 100 bar (middle) and ammonia at 50 bar (right). The decompressions from pressure liquefied initial conditions therefore involve an isentropic decompression to saturated liquid condition, followed by an isenthalpic saturated two-phase decompression. The polytropic approximation is fitted to the two-phase section of the decompression. For the gas initial conditions (e.g. carbon dioxide with $T > 330$ K), the decompression trajectory is a good approximation of the CoolProp prediction with $m = 1$ which is indicative of isothermal ideal gas behaviour. Decompressions from pressure liquefied initial conditions are characterised by an initially weakly compressible isentropic expansion to saturated conditions, with the subsequent isenthalpic decompression being qualitatively captured by the polytropic approximation. Whilst the approximation does not appear to be accurate throughout the range of pressures (generally predicting larger densities at low pressures), it has the property of precisely reproducing the integral of density with respect to pressure over the mathematically convenient range between zero and the initial pressure. A user without access to CoolProp may implement the method by using, or interpolating between, the values of m given in Figure 2 for pressure liquefied substances, or by choosing $m = 1$ for ideal gas conditions. The initial density can be calculated using the CoolProp online calculator or another appropriate method. The average density ($\bar{\rho}$) can be evaluated using the Gamma function in Microsoft Excel or another package given a suitable pipe index value.

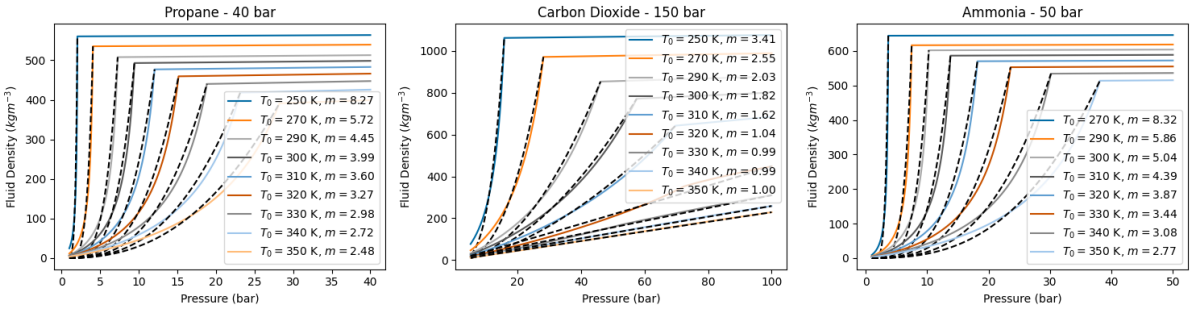

Figure 2 Comparison of the CoolProp decompression (coloured lines) with the approximate polytropic decompression calculated for: propane (left), carbon dioxide (middle) and ammonia (right). Cases which are pressure liquefied are decompressed isentropically to a 100% liquid condition before an isenthalpic decompression to atmospheric conditions. Gas cases are decompressed isenthalpically to atmospheric conditions. The polytropic index (m) is calculated using (26).

[5] This is notable because the polytopic exponent is chosen to satisfy a physical constraint and is not an empirically determined factor.

[6] PolyPiRRaM utilises CoolProp to calculate all thermophysical properties using Helmholtz equations of state for pure substances.

Extending the transient solution to the pressure and temperature on the release plane is relatively straight forward. All that is necessary is to find the pressure corresponding to the mass flux density on the release plane. This can be done analytically for ideal gases, whereas real gases and choked two-phase scenarios will require numerical methods.

The model predicts an infinite initial mass flow rate, which is undesirable. Consequently, the maximum mass flow rate is capped by the corresponding maximum choked mass flow rate ($Q_{\max}$), which is taken to be either the ideal gas choked flow rate, or the Webber et al. (1999) flow rate[7] for flashing releases. The capping is applied assuming mass conservation which causes the solution to be slightly delayed.

Sensitivity Analysis

Gaussian emulation modelling is a convenient approach to assess the model sensitivity to variation in input parameters. The input parameters are assumed to be subject to a $\pm$10% variation around a base case, with Latin-hypercube sampling (LHS) used to generate a database of input conditions around a base case. The model is then run on the LHS input dataset creating a second dataset which upon which the Gaussian emulator can be trained using GEM-SA (Kennedy et al., 2006; O'Hagan, 2006). This enables model's sensitivity to variation in the different parameters to be inferred. Four base cases are analysed using a mass flow rate value taken from a point in the early and late time regimes of gas and pressure liquefied fluid releases. Figure 3 and Figure 4 show sensitivity analysis for gas (methane) and pressure liquefied (propane) releases respectively. The left-hand and right-hand figures show the sensitivity of the early time regime, and late times respectively. Each plot is a bar chart in which the height of the column for each parameter corresponds to the proportion of the total variance that can be attributed to that variable. Orange shading corresponds to the role of interactions with other parameters. The grey line/zone shows the cumulative proportion of variance which is explained by the variables.

These figures match an intuitive expectation of pipeline decompression sensitivity to different parameters. The most important variable in each case is the pipeline diameter, which explains between 70 % and 80% of the total variance. Fortunately, the pipeline diameter is likely to be known for any scenario. The second most important parameter depends on the case being modelled. For gas releases, the pressure is the next most significant variable, explaining approximately 20% of the model variance followed by the temperature. For pressure liquefied releases the initial temperature is the second most important parameter and the pressure has a negligible effect. This difference is expected and is due to the isentropic decompression to saturated conditions which is assumed for pressure liquefied cases. In the early time limit, the remaining parameters, surface roughness, atmospheric pressure and pipe length play almost negligible roles which is expected for modelling a pipeline during the early stages of the release. In the late time limit, the pipe length plays a marginally more significant role, due to the pipe length affecting the transition mass and time. To summarise, the sensitivity analysis indicates that the model behaves in a manner that is expected, given the design of the model. In which case, the analysis provides assurance that the model is working as intended.

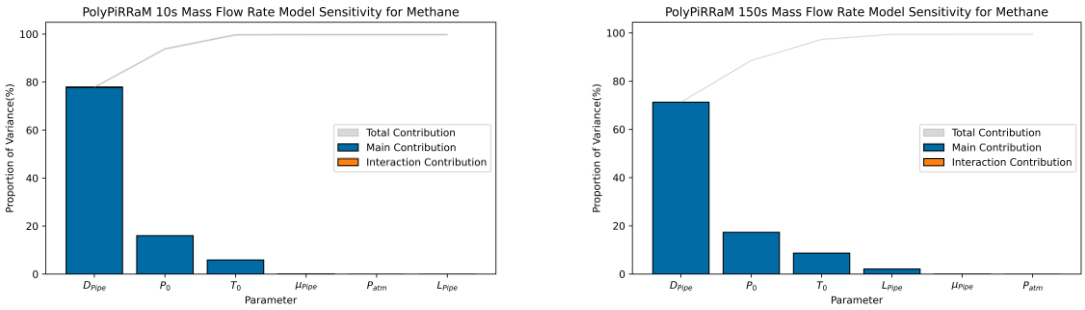

Figure 3 Model sensitivity for the mass flow rate using gaussian emulation for a gas release. The base case is a full-bore rupture of an 8 km long, 150 mm diameter pipeline with 45 μm surface roughness, transporting methane at 15 °C and 100 bar. The plots show sensitivity analysis at arbitrary times corresponding to the early and late decompression regimes. Input variables are assumed to be subject to a 10% variability.

[7] Defining $\phi(T) = \frac{h_{\mathrm{liq}}(T) - h_{\mathrm{vap}}(T)}{v_{\mathrm{liq}}(T) - h_{\mathrm{vap}}(T)}$, Webber et al. (1999) derives the two-phase choked liquid mass flow rate as $G_{\mathrm{max,2phase}} = \frac{\phi(T)}{\sqrt{c_p T - \phi(T) v_{liq}}}$ which is easily evaluated using CoolProp. For temperatures exceeding $0.95T_{\mathrm{crit}}$ this approach is found to be non-conservative, and the mass flux density calculated at $0.95T_{\mathrm{crit}}$ is used instead.

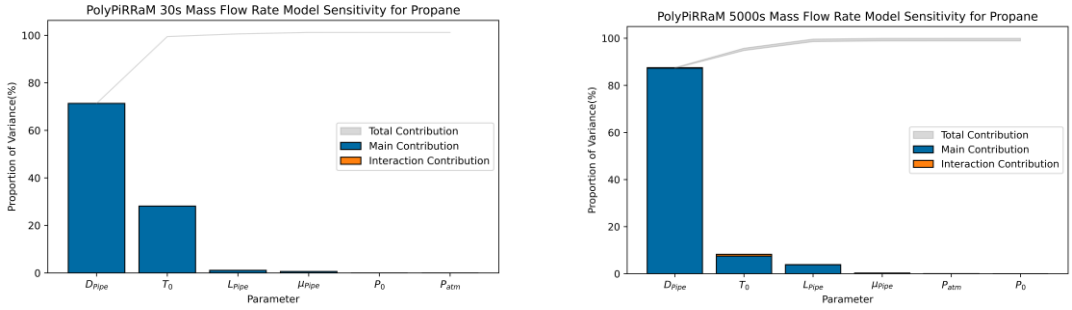

Figure 4 Model sensitivity for the mass flow rate using gaussian emulation for a pressure liquefied fluid release. The base case is a full-bore rupture of an 8 km long, 150 mm diameter pipeline with 45 µm surface roughness, transporting propane at 15 °C and 50 bar. The plots show sensitivity analysis at arbitrary times corresponding to the early and late decompression regimes. Input variables are assumed to be subject to a 10% variability.

Model Intercomparison

Figure 5 and Figure 6 show comparisons between mass flow rate predictions from PolyPiRRaM and PHAST for gaseous and pressure liquefied initial conditions. PolyPiRRaM predictions are plotted using orange lines, and PHAST predictions are shown using blue lines. All predictions relate to a single pipe opened at one end. Figure 5 (left) shows the transient mass flowrate predictions for an 8 km long, 150 mm diameter pipeline transporting methane at 100 bar, and 20 °C, with Figure 5 (right) displaying the mass flow rate predictions corresponding to an 16 km long, 150 mm pipeline transporting hydrogen at 100 bar and 20 °C. The agreement between the PHAST and PolyPiRRaM predictions for these cases is very good, demonstrating that the PolyPiRRaM model is a good approximation to the underlying conservation equations.

Figure 6 (left) shows the transient mass flow rate predictions for a pipeline transporting propane in an 8 km long, 500 mm diameter pipe at 13.5 bar, and 30 °C. Figure 6 (middle) shows the transient mass flow rate predictions for a pipeline transporting ammonia in an 8 km long, 150 mm diameter pipe at 31 bar, and 30 °C. Figure 6 (right) shows the transient mass flow rate predictions for a pipeline transporting carbon dioxide ruptured midway along a 96 km long, 600 mm diameter pipe at 150 bar, and 30 °C. The propane and ammonia releases are at relatively low temperatures in comparison to the critical point, whereas the carbon dioxide case is close to the critical temperature and at a supercritical pressure. The transient predictions for pressure liquefied fluids are quantitatively very similar, with PolyPiRRaM generally predicting slightly larger mass flow rates. Given the variation due to alternative equation of state modelling, (i.e., Peng Robinson in PHAST vs polytropic approximation to the Helmholtz EOS modelling in PolyPiRRaM) the difference between predictions is acceptable.

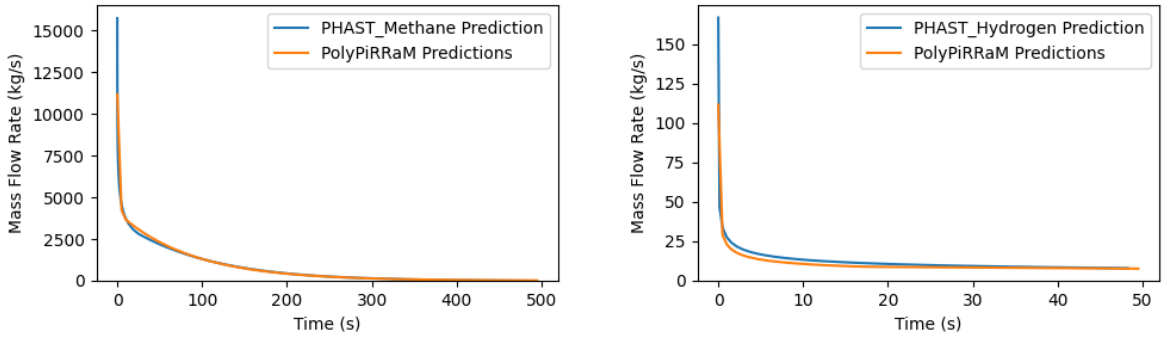

Figure 5 PolyPiRRaM predictions for the mass flow rate for gaseous initial conditions shown in comparison to PHAST GasPipe predictions for an 8km pipeline transporting methane (left) and a 16km pipeline transporting hydrogen (right).

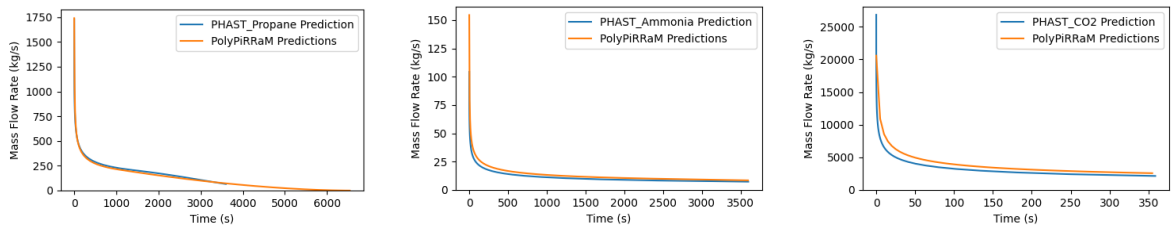

Figure 6 PolyPiRRaM mass flow rate predictions for pressure liquefied initial conditions shown in comparison to a PHAST V9.1 PipeBreak predictions for a pipeline containing propane (left), ammonia (middle), and CO_2 (right).

Model validation

Gas Comparisons

Figure 7 presents mass flow rate predictions from PolyPiRRaM in comparison to experimental measurements of full-bore ruptures to pipelines containing natural gas. Comparisons to the large-scale APIGEC trials using air are shown in the left and middle plots, with comparisons to the reduced scale experiment of Norris (1994) shown in the right plot. PolyPiRRaM predictions are plotted using the orange line, and the experimental measurements are plotted with the blue line.

The quantitative agreement between the experimental measurements and the model predictions is good. It appears that the experiments are unable to record the rapid variations in mass flow rate that occur at the beginning of the releases, and the PolyPiRRaM predictions are significantly larger than the measurements, but this is reasonable given the duration of the release. In particular, the Norris full-bore rupture data is reported as numerical constants (K_1 and K_2) describing the exponential decay profile ($\dot{M} = K_1 e^{-K_2 t}$). This unfortunately would have the effect of smoothing the rapid transient effects at the beginning of the release. At the later stage of the release the decay is predicted well, with particularly good agreement in the Norris experiment, where the whole experimental apparatus, a 600 m coil of 10 mm high pressure piping, was sufficiently compact to be continuously weighed during the release.

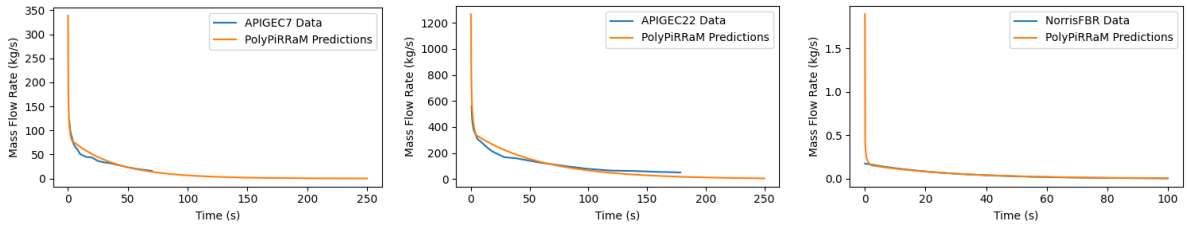

Figure 7 Comparison of PolyPiRRaM mass flow rate predictions to the APIGEC7 (left) and APIGEC22 (middle) air experiments, and the Norris FBR (right) methane experiment.

Pressure Liquefied Fluid Comparison

Figure 8 shows inventory predictions from PolyPiRRaM in comparison to a subset of the Isle of Grain experimental measurements of full-bore ruptures to pipelines containing propane. Comparisons of PolyPiRRaM predictions to the 150 mm internal diameter and 100 m long Isle of Grain P40 experiment are shown in the Figure 8 (left), and to the 50 mm internal diameter and 100 m long IoG P61 experiment are shown in Figure 8 (right). PolyPiRRaM predictions are plotted using the orange line, and the experimental measurements are plotted with the blue line.

The agreement between the experimentally measured inventory and the model predictions is quantitively good throughout the release.

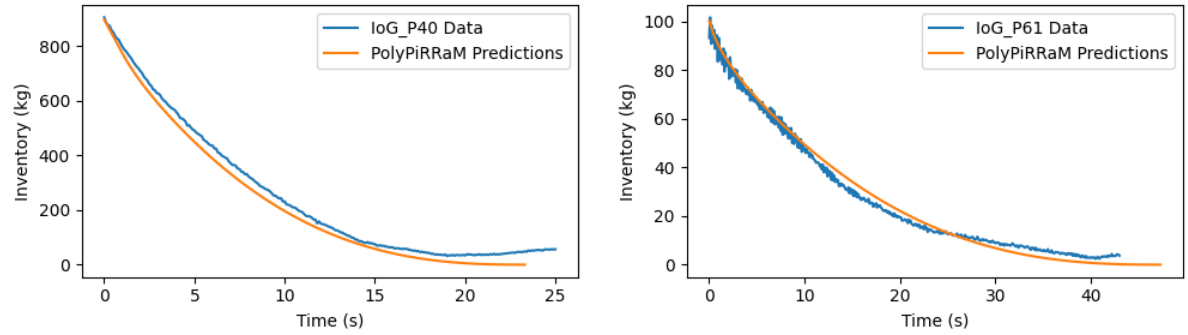

Figure 8 PolyPiRRaM Mass flow rate predictions for the Isle of Grain P40 (left) and P61 (right) trials shown in comparison to the experimental data.

Summary

A new analytical solution to the compressible quasi-steady pipe-flow equations has been derived. The new model predicts a previously undiscovered scaling law associated with the non-reacting discharge of compressible flows from pipes. Specifically, the mass flow rate ($\dot{M}$) is predicted to decay to the minus one-third power of time ($\dot{M} \propto t^{-\frac{1}{3}}$) during the early stage of the release. That is, the mass flow rate is halved when the time after the release is eight times longer (i.e. if the mass flow rate is 100kg/s at 10 s after the rupture, it will reach 50 kg/s at 80 s after the rupture). This is particularly novel, as the scaling law appears to be a ubiquitous property of compressible flow escaping pipes. In which case, the model developed here is applicable to a wide class of releases and can be adapted between gas and pressure liquefied releases by changing material specific parameters (i.e. the initial density, polytropic index and viscosity).

The new model is thoroughly tested using gaussian emulation sensitivity analysis which reveals no unexpected behaviour, whilst confirming the expected sensitivity of the model predictions to uncertainty in the model input parameters. Comparison

to DNV's PipeBreak model in PHAST for a series of gas and pressure liquefied fluid releases shows that PolyPiRRaM makes comparable mass flow rate predictions to the more established model. Validation comparisons to experimental data for both gas (air and methane) and pressure liquefied fluid (propane) releases demonstrates how the new approach is capable of quantitatively capturing the transient decay of the mass flow rate. Due to space limitation in this publication, exhaustive comparisons are not possible to include, but additional comparisons have demonstrated good performance of the model. Here, the comparisons presented have been chosen to demonstrate the key capabilities of the model across a range relevant full-bore rupture scenarios.

The model as described in this paper predicts only the inventory/released mass, and the mass release rate for a rupture at the end of a single pipe. The upstream and downstream orifice temperature and pressure can be also predicted with a little ingenuity. For example, the combination of assuming an isenthalpic expansion[8] into a choked or non-choked mass flow rate is sufficient to deduce the likely orifice conditions (pressure, temperature, vapour quality). In the late-time regime the upstream pressure can be evaluated using (14), and the upstream temperature can be inferred assuming an appropriate expansion process. Releases at arbitrary positions along a pipeline can be modelled by considering two independent releases and summing the result.

In principle the new solution can be extended to include the effect of liquid compressibility and pumping, which future work may address. PolyPiRRaM can also be used to model supercritical fluid releases, although there is uncertainty about choosing appropriate pipe index values (n). The underlying PolyPiRRaM solution is robust, and appropriate values for the pipe index (n) are known a-priori for gas and two-phase releases, however, a framework for supercritical fluid releases has not yet been fully established. There are various approaches which may be adopted: the simplest approach pragmatically assumes releases decompressing to 100% liquid have $n = 0$, after an isotropic decompression to saturated conditions, and all other releases are presumed to have $n = 2$. This is likely to be an acceptable solution for most release scenarios. Though there is likely to be a discontinuity at the point of transition between the models. However, the isentropic decompression to pseudocritical conditions will likely incur a significant density change. In which case, some sort of liquid compressibility modelling may then be required. It may be the case that incorporating the liquid compressibility might be enough to provide a smooth transition into gas-like flow, though this may require numerical integration.

Extending the model to holes may be possible during the first few percent of mass lost using rescaling techniques, however, a full analytical solution for small holes may not be possible, though approximations may deliver acceptable approaches. In which case, it is probably simplest to solve the quasi-steady compressible pipe flow equations numerically, or implement a Godunov type solver to tackle the fully non-linear system (Shargatov et al., 2019). Multicomponent releases, for example spiked crude with water, can also be modelled provided that an appropriate equation of state can be identified.

To summarise, the new model has been demonstrated to be capable of modelling a wide range of pressure liquefied full bore rupture releases. In the first instance, the model serves as a useful verification test case for complex numerical tools where exhaustive testing is useful to find implementation inconsistencies. PolyPiRRaM may also find use where simple tools are required to quickly model release scenarios, possible for land use planning or loss prevention activities. The new model predicts transient mass release rates for full-bore ruptures to pipelines, across a wide range of scenarios. PolyPiRRaM can be applied to releases of pressure liquefied substances (ammonia, dense phase carbon dioxide, ethylene, cryogenic liquid hydrogen, and propane) and gas releases (natural gas, light phase carbon dioxide, and ambient temperature hydrogen). The application is not restricted to pipelines on land, as subsea releases can be modelled provided the water depth is sufficiently shallow to enable a sufficiently large density change along the pipe.

Authorship

The author confirms sole responsibility for the following: study conception and design, data collection, analysis and interpretation of results, and manuscript preparation.

Acknowledgements

The author gratefully acknowledges Zoe Chaplin and Liam Gray from HSE, and Gemma Tickle of GT Science, for their editorial and technical comments which have helped improve the manuscript.

Disclaimer

This publication and the work it describes were funded by the Health and Safety Executive (HSE). Its contents, including any opinions and/or conclusions expressed, are those of the authors alone and do not necessarily reflect HSE policy.

[8] The isenthalpic decompression should be from the initial conditions if gas, and from saturated liquid conditions following an isentropic decompression from pressure liquefied fluid initial conditions.

References

APIGEC. (1979). Hydrogen Sulphide Isopleth Prediction, Phase 2, Pipe Burst Study.

Bell, I. H., Wronski, J., Quoilin, S., & Lemort, V. (2014). Pure and pseudo-pure fluid thermophysical property evaluation and the open-source thermophysical property library CoolProp. Industrial & engineering chemistry research, 53(6), 2498-2508.

Bell, R. (1978). Isopleth calculations for ruptures in sour gas pipelines. Energy Processing/Canada, 36.

Betteridge, S. (2023). Shell FRED 2023 Technical Guide Technical description of hazard consequence models (Fire, Release, Explosion, Dispersion) in FRED (INTERNAL – SRN--04582). Shell Research Limited.

Chaplin, Z. (2015). Rewriting MISHAP: The development of MISHAP12. (RR1040). Retrieved from http://www.hse.gov.uk/research/rrhtm/rr1040.htm

Fannelop, T., & Ryhming, I. (1982). Massive release of gas from long pipelines. Journal of Energy, 6(2), 132-140.

Haaland, S. E. (1981). Simple and Explicit Formulas for the Friction Factor in Turbulent Pipe Flow, Including Natural Gas Pipelines. Univ., Norwegian Inst. of Technol., Division of Aero-and Gas Dynamics.

Jones, R., Lehr, W., Simecek-Beatty, D., & Reynolds, M. (2013). ALOHA® (Areal locations of Hazardous Atmospheres) 5.4. 4: technical documentation.

Kennedy, M. C., Anderson, C. W., Conti, S., & O'Hagan, A. (2006). Case studies in Gaussian process modelling of computer codes. Reliability Engineering & System Safety, 91(10-11), 1301-1309.

Lees, F. (2012). Lees' Loss prevention in the process industries: Hazard identification, assessment and control. Butterworth-Heinemann.

Martynov, S. B., Porter, R. T., & Mahgerefteh, H. (2024). Estimating the line packing time for pipelines transporting carbon dioxide. Carbon Capture Science & Technology, 11, 100188.

Newton, A. (2022). Pipeline Release Rate Model for pressure liquified flows. Hazards 32, Symposium Series. https://www.researchgate.net/publication/365623566_Pipeline_Release_Rate_Model_PiRRaM_for_Pressure_Liquefied_Gases

Norris, H. L. (1994). Hydrocarbon blowdown from vessels and pipelines. SPE Annual Technical Conference and Exhibition,

O'Hagan, A. (2006). Bayesian analysis of computer code outputs: A tutorial. Reliability Engineering & System Safety, 91(10-11), 1290-1300.

Richardson, S., & Saville, G. (1996). Isle of Grain pipeline depressurisation tests. (OTH-94-441).

Shargatov, V. A., Sumskoi, S. I., & Pecherkin, A. S. (2019). Simulation of gas release from pipelines using a new numerical method based on the Godunov approach. Journal of Physics: Conference Series, 1205(1), 012050. https://iopscience.iop.org/article/10.1088/1742-6596/1205/1/012050/pdf .

Tam, V., & Higgins, R. (1990). Simple transient release rate models for releases of pressurised liquid petroleum gas from pipelines. Journal of hazardous materials, 25(1-2), 193-203.

Van den Bosch, C., & Weterings, R. (2005). Methods For The Calculation Of Physical Effects Cpr14e. Yellow Book, Comimittee For The Prevention Of Disasters, 3rd Ed., Nl.

Webber, D., Fannelop, T., & Witlox, H. (1999, September). Source terms from two-phase flow in long pipelines following an accidental breach. International Conference and Workshop on Modelling the Consequences of Accidental Releases of Hazardous Materials, CCPS, San Francisco, California.

Wilson, D. J. (1979 (Re-issued 1986)). Release and Dispersion of Gas from Pipeline Ruptures. Alberta Environment.

Yu, S., Yan, X., He, Y., Chen, L., Yu, J., & Chen, S. (2024). A new model to predict the small-hole decompression process of long CO2 pipeline. Process Safety and Environmental Protection, 187, 443-458.

Zelensky, M. J., & Zelt, B. W. (2010). ERCBH2S, A Model for Calculating Emergency Response and Planning Zones for Sour Wells, Sour Pipelines and Sour Production Facilities. Energy Resources Conservation Board.